SURFACE AND INTERFACE ANALYSIS, VOL. 15, 405–414 (1990)

Monte Carlo Calculations of the X-ray Induced Enhancement Signal in Electron Probe Microanalysis (EPMA) and Auger Electron Spectroscopy (AES) of Stratified Materials

A. G. Nassiopoulos and E. Valamontes
Microelectronics Institute, NCSR 'Demokritos', PO Box 60228, 153 10 Aghia Paraskevi Attikis, Athens, Greece

When thin overlayers on a bulk material have to be analysed by EPMA (electron probe microanalysis) or AES (Auger electron spectroscopy), the signal obtained is enhanced by three factors: (i) back-scattering, (ii) characteristic x-rays induced in the bulk by the primary beam and (iii) continuous x-rays (bremsstrahlung) created also in the bulk. The Monte Carlo techniques are applied in order to evaluate the above three enhancement factors when the primary energy is varied in the range 5–50 keV. It is shown that at high primary energies the second and third factors are no longer negligible and become significant in some cases. The approximation to ignore the third factor in EPMA and both the second and third factors in AES is not always valid and introduces an appreciable error. Results are shown for the case of thin films (Al, Au, Cu) on a bulk material (Au, Cu, Si, Ni, Pt).

INTRODUCTION

Electron probe microanalysis (EPMA) and Auger electron spectroscopy (AES) are two techniques that are based on the same primary mechanism of electron-induced ionization. The difference resides in the secondary mechanism of de-excitation of the atoms, which is, in the first case, x-ray emission and, in the second case, Auger electron emission. This difference introduces a great difference in the analysed volume, the depth of which is limited in the case of AES to some tens of angstroms as opposed to that of the EPMA technique, which may attain some microns at high primary voltages (of the order of 30–40 keV). But when very thin overlayers on a bulk material have to be analysed, the analysed depth is imposed by the thickness of the film, so it is approximately the same in the two cases.

In both techniques (EPMA and AES) the signal induced by the primary electron beam is enhanced by that induced by back-scattered electrons and by characteristic and continuous x-rays created in the bulk by the primary beam. In quantitative EPMA only the first two factors are usually taken into account (back-scattering coefficient and fluorescence correction due to characteristic x-rays).[1–8] The third factor is considered to be negligible. This is indeed valid when we have bulk materials, as shown by the detailed calculations of Henoc[9] and Henoc and Maurice[10] and the experimental results of Castaing and Descamps.[11] Thus, even recent models for data processing in quantitative x-ray microanalysis, such as those based on a ZAF structure (Love and Scott's model[12]) or those based on a $\varphi(\rho z)$ approach (Brown and Packwood's model[13]), neglect the fluorescence correction due to the continuum. In some cases of stratified materials this approximation is no longer valid, as will be shown by our results below. Recently, a modified PAP model (which is a model based on both the ZAF model and the $\varphi(\rho z)$ approach[6]) for stratified materials uses analytical expressions in order to calculate the fluorescence contribution by the continuum in the case of thick layers on a substrate.[14] Our calculations use Monte Carlo methods in order to evaluate the fluorescence correction by both characteristic and continuous x-rays in the case of very thin overlayers.

In AES when a conventional Auger apparatus is used (primary beam energy in the range of 3–5 keV), the only correction factor taken into account is that due to back-scattering. This correction is achieved by using more or less sophisticated methods. The Auger signal induced by x-rays created in the bulk by impinging electrons is often neglected, although some authors have mentioned the contribution of this effect to the total signal.[15–20] With the new generation of Auger instruments using a primary beam energy of 50–100 keV (field emission gun), the above approximation is no longer valid. In this case, the enhancement due to back-scattering is important but also the contribution of continuous and characteristic x-rays from the bulk is no longer negligible. The first numerical evaluation of the contribution of characteristic and continuous x-rays from the bulk to the Auger signal was carried out by Cazaux and Moutou,[21,22] who used analytical formulae.

In this article, Monte Carlo techniques have been used in order to evaluate the contribution of both the back-scattered electrons and continuous (bremsstrahlung) and characteristic x-rays, created in the bulk, to the total signal in EPMA and AES of thin overlayers (Al, Au, Cu) on a bulk material (Au, Cu, Si, Ni, Pt). Correction factors have been calculated that may be used in quantitative AES and EPMA of stratified materials.

0142-2421/90/070405–10 $05.00

Received 8 September 1989
Accepted 1 February 1990

GENERAL FORMALISM

As described earlier, the signal collected in AES and EPMA results mainly from three factors:
(1) the incoming electron beam;
(2) energetic back-scattered electrons;
(3) characteristic x-rays created in the bulk by the incoming and by back-scattered electrons;
(4) the bremsstrahlung produced in the bulk.
We neglect here auto-ionization in the sample.

When thin unsupported films have to be analysed, only the first factor is important. The other three factors become negligible if the thickness of the film is sufficiently small. On the other hand, when the same film is supported by a bulk material, back-scattering and x-rays created in the substrate contribute to the enhancement of the signal produced in the film by the incoming electrons. Thus, by comparing the signals obtained in these two cases, we have a direct method to obtain the enhancement factors due to all the above contributions. The signal from a thin unsupported film is compared to that from a film of the same thickness on a bulk material. The signal from the unsupported film is supposed to be equal to that due only to the primary beam in the second case.

The above method of obtaining the enhancement factor has been used experimentally, firstly by Gramari and Cazaux[23] in AES measurements and later by El Gomati[24,25] in EPMA measurements. The same idea may be used in calculations. We have used this method in order to normalize our results obtained by Monte Carlo calculations.

The total signal I_t is written in the form

$$I_t = I_p + I_b + I_{ch} + I_{co} = I_p(1 + I_b/I_p + I_{ch}/I_p + I_{co}/I_p) \quad (1)$$

where I_p is the signal due to the incoming beam, I_b that due to back-scattered electrons, I_{ch} that due to characteristic x-rays from the bulk and I_{co} that due to the bremsstrahlung from the bulk.

The signal I_p due to the incoming electrons is equal, as explained above, to the signal I_f from a thin unsupported film. Thus, it is calculated by using the Monte Carlo program on an unsupported film of thickness 400 Å. The thickness of 400 Å has been proved to be sufficiently small in order to avoid back-scattering within the film for the energy range used here (5–50 keV). The total signal from a film of the same thickness as the unsupported one on a bulk material is then evaluated and each individual factor is normalized to the signal $I_f(=I_p)$ obtained from the thin film.

As the initial mechanism in both cases (AES and EPMA) is the excitation of a core level and as a ratio of two signals is considered, one from a thin unsupported film and the other from a film of the same thickness on a bulk material, all the constants (fluorescence or Auger yield, transparency of the spectrometer, etc.) are cancelled-out, so the only difference in the two cases lies in the difference of the range of x-rays and Auger electrons created. Indeed, for the film thickness used (400 Å) almost all the x-rays created within the film come out of it (the attenuation is negligible), but this is not so in the case of Auger electrons. For this last case we have considered that the attenuation is exponential, so a signal created at a depth X has to be multiplied by $\exp(-X/\lambda \cos\theta)$, where λ is the electron attenuation length for electrons of energy E_{ijk} (= energy of Auger electrons from the levels i, j, k) and $\theta = 42°$ (for a cylindrical mirror analyser).

MONTE CARLO PROGRAM

The basic computation model for the calculation of electron trajectories is similar to that used previously by other authors.[12,26,27] It is based on the following assumptions:
(1) Elastic scattering is described by a screened Rutherford cross-section.
(2) Angle deviation is considered to be only due to elastic scattering. This is close to reality, as inelastic scattering occurs through very small angles.
(3) Between two scattering points, electrons are considered to lose energy continuously.
(4) Each step length for elastic scattering is considered to be constant and equal to 1/100 of the total electron range (plural scattering model[12]). The total length of the electron trajectory within the sample is taken to be the Bethe range. With this approximation, the calculation time is reduced significantly while little error is introduced.

Along each step length of the electron trajectory between elastic scattering positions, the Bethe continuous energy-loss formula is used, given by[28]

$$dE/ds = -78\,500\rho Z \ln(1.166E/J)/AE \text{ (keV cm}^{-1}) \quad (2)$$

where s is the electron path, ρ (g cm^{-3}) the density of the target, Z the atomic number, A (g) the atomic weight, E (keV) the energy of incident electrons and J the mean ionization potential, which is given as a function of the atomic number by the equation[29]

$$J = (9.76Z + 58.5/Z^{0.19}) \text{ (eV)} \quad (3)$$

The Bethe equation describes well the energy loss in the target for high energies, but it cannot be extended to energies for which $E < J/1.166$ since the logarithmic term of Eqn (2) becomes negative. For those energies ($E < 6.4J$), the expression of Rao-Sahib and Wittry[30] is used, which is the parabolic extrapolation to $E = 0$ from below the inflection point of the Bethe expression at $E = 6.4J$. Thus, for $E < 6.4J$ Eqn (1) is replaced by

$$dE/ds = -62\,400\rho Z/A(EJ)^{0.5} \text{ (keV cm}^{-1}) \quad (4)$$

The total back-scattering coefficient is calculated at the end of each sequence of trajectories as a mean to test the convergence of the program. As mentioned above, the program is run for two cases: a thin unsupported film and a thin film (same thickness as the unsupported one) on a bulk material.

The ionization mechanisms involved are:
(1) ionization in the film from incoming and back-scattered electrons
(2) ionization from characteristic x-rays created in the substrate by impinging electrons
(3) ionization by continuous x-rays (bremsstrahlung) also created in the substrate by passing electrons.

We will consider separately the cases of EPMA and AES.

EPMA signal

Different contributions to the signal

EPMA signal induced by incoming and back-scattered electrons. This signal is calculated as follows. The electron range is divided into 100 steps. Elastic scattering occurs at the beginning and end of each step. In order to calculate the energy loss, each step is divided into 100 smaller steps and the energy is calculated at the end of each step.

At each small step, the energy and position of the electron is known, so we can calculate the x-ray signal at each step using the formula

$$I_1 = (\rho \cdot N/A) \cdot \sigma(E) \cdot \text{step} \cdot \omega_{ij} \qquad (5)$$

where $\sigma(E)$ is the ionization cross-section given by the Gryzinski's formula, ρ and A are the density and atomic weight, respectively, ω_{ij} is the fluorescence yield and N is Avogardro's number.

The x-ray signal comes only from the film. When the electron passes into the substrate it changes its scattering and energy-loss parameters. If it re-enters the film after back-scattering, it is considered again to create x-rays if it has enough energy (higher to the binding energy of the level of interest).

The calculated signal is arranged in a 1×100 matrix according to its position of creation in the film (the film thickness is divided into 100 layers). The total signal is then calculated by summing all separately calculated signals (term $1 + I_b/I_p$ in Eqn (1)).

EPMA signal induced by characteristic x-rays from the substrate (term I_{ch}/I_p in Eqn (1)). Characteristic x-rays created in the substrate by propagating electrons are calculated as explained above. The x-ray emission is considered to be isotropic and a random number is considered for the emission angle of these x-rays. A part of them is absorbed within the substrate (approximately half of them) and another part enters, after absorption correction, into the film. Their path length within the substrate and the film is calculated by considering their emergence angle θ (path length $= t/\cos\theta$, where t is the length corresponding to $\theta = 0$ and θ is taken randomly). The EPMA x-ray signal is calculated at each of the 100 layers of the film by considering the probability that x-rays entering the layer are absorbed by the layer on their way out of the film. Absorption correction of the x-ray signal created within the film is also considered, although negligible for the film thickness used. The number of 100 layers used is also excessive for the absorption within the film, but it is convenient because we continue the same division as that used for the electron-induced signal. The calculated signal is indicated by I_{ch}/I_p in Eqn (1). The absorption coefficients used are taken from the x-ray cross-section compilation from the Kaman Science Corporation.[31]

EPMA signal induced by continuous x-rays from the substrate. The approximation made is as follows. We consider that continuous x-rays are all created at the film/bulk interface by incoming electrons. We have considered the interface and not the surface of the film owing to the infinitely small thickness of the film used. The continuous spectrum is then calculated by using Dyson's formula[32]

$$g(h\nu) = 2.76 \times 10^{-9} Z(E_0/h\nu - 1) \qquad (6)$$

where $g(h\nu)$ is the number of photons of energy $h\nu$ per electron per electron-volt, Z is the atomic number and E_0 is the energy of the incoming electron.

Half of the created continuous photons are considered to enter the film and create an EPMA signal. This is a rough approximation because it is known that continuous x-ray emission is not isotropic but is more probably oriented in the direction of the electrons that create this radiation. A better approximation complicates the problem significantly. The ionizations in the film due to continuous x-rays are calculated for every sublayer (1/100 of the total thickness) and for all the energy spectrum of created photons. This spectrum is divided into energy intervals differing by 100 eV from each other. X-ray ionization cross-sections are taken by fitting on the curves given in the x-ray cross-section compilation book.[31] Absorption correction is also considered, although not significant.

Area from which the signal originates. It is particularly important to know if, in the case of stratified materials, the lateral extent of the back-scattered and fluorescence contribution to the EPMA signal limits the spatial resolution in x-ray microscopy, as occurs in the case of bulk materials. In this respect, we have calculated the lateral distribution of the x-ray signal from the primary beam in comparison with the signal from all the other contributions. Results will be given below, showing that the lateral resolution of x-ray microanalysis in the case of thin overlayers is principally governed by the extent of the signal due to the primary beam, in agreement with experimental results by Jbara *et al.*[33] This result is expected if we take into account that x-ray microanalysis of thin overlayers is analogous to AES, where this result seems to be well established.[34–36]

AES signal

The only difference in considering the AES signal with respect to the EPMA signal is due to the different mean free path of Auger electrons with respect to x-rays. The corresponding difference in the signal is minimized in the case of very thin films. In our case, the thickness of the film is 400 Å, which is still greater than the mean free path of Auger electrons (of the order of some tens of angstroms), so a small difference subsists.

The formula for Auger electrons is given by

$$I_{\text{Auger}} = (\rho \cdot N/A) \cdot \sigma(E) \cdot \text{step} \cdot a_{ijk} \times \exp(-X/\lambda \cdot \cos\theta) \qquad (7)$$

where a_{ijk} is the Auger yield, X is the position of creation of the Auger electron, λ is the electron attenuation length and θ is the escape angle ($\theta = 42.3°$ when a cylindrical mirror analyser (CMA) is used).

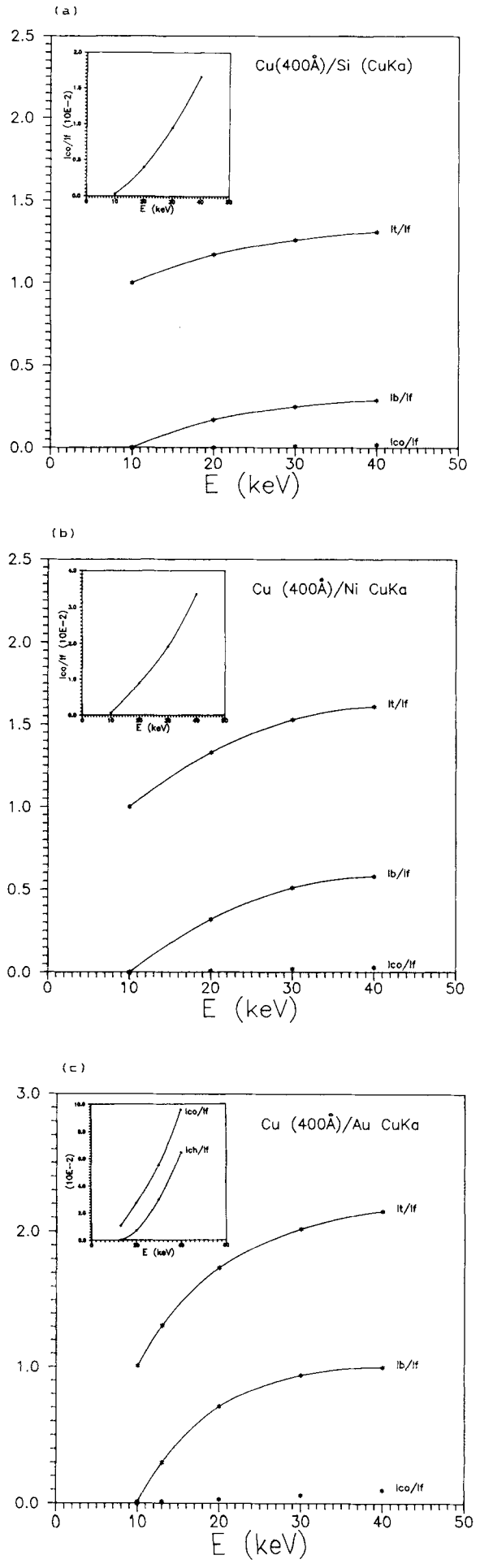

RESULTS AND DISCUSSION

Figures 1–4 indicate the results obtained from Monte Carlo calculations when an x-ray signal is detected. In these figures, I_t/I_f is the ratio of the total EPMA signal to the signal obtained from the thin unsupported film. As mentioned above, the signal from the thin unsupported film is practically created only by the primary beam, so $I_f = I_p$; I_b/I_f is the back-scattering correction factor, given as the percentage of the signal due to back-scattered electrons with respect to that created by the primary electrons; I_{ch}/I_f is the percentage of the signal due to characteristic x-rays from the substrate and I_{co}/I_f is that due to continuous x-rays also from the substrate.

In Fig. 1, a copper film (thickness t = 400 Å) has been used on different substrates and the Cu Kα line has been considered. It is seen that when the substrate is a low Z material, the total signal ratio after correction does not exceed 1.3 at 40 keV. This ratio increases to 1.6 at 40 keV when the substrate is Ni (Z = 28) and to 2.2 when the substrate is Au (Z = 79). The correction due to continuous x-rays from the substrate passes from 2% for a Si substrate to 10% for an Au substrate (insert of Figs. 1(a)–(c)).

When the Cu Lα line is detected, this correction factor reaches 13% for an Au substrate (Fig. 2). The contribution of characteristic x-rays is important in the case of Cu/Si (8%).

For an aluminium overlayer (Fig. 3, t = 400 Å, detection of Al Kα), the correction factor due to characteristic x-rays takes large values in the case of silicon (of the order of 19% at 40 keV). This is due to the fact that characteristic x-rays from silicon (Si Kα) act with a favourable cross-section, as they are situated close in energy to the binding energy of Al. Continuous x-ray correction does not exceed 7% for all the substrates used.

In the case of an Au overlayer (Fig. 4), the continuous x-ray correction reaches very large values for high Z substrates (10% at 40 keV when the Au Lα line is detected for a Pt substrate, and 11% when the Au Mα line is detected for the same substrate). Characteristic x-ray correction is, in this case, small.

In general, the total correction factor increases when the Z value of the substrate increases (see Fig. 5). It reaches values as large as 2.5 (Cu Lα, Cu/Au) for E_0 = 40 keV. It depends on the x-ray signal detected and this is due to the different cross-sections for the corresponding energy levels and to a small difference due to absorption.

In Fig. 6, published experimental results by Cazaux *et al.*,[37,38] giving the total enhancement factor $I_t/I_f = 1 + R_{A/S}$ (A = analysed element of the overlayer; S = substrate), are compared to our results. The experi-

Figure 1. Monte Carlo calculations of the different contributions to the x-ray signal as a function of energy for a Cu overlayer (400 Å thick) on different substrates: (a) Si; (b) Ni; (c) Au. Cu Kα radiation has been considered. I_t/I_f = ratio of the total signal from the overlayer to the signal from a thin unsupported film. I_b/I_f = enhancement factor due to back-scattered electrons; I_{ch}/I_f = enhancement factor due to characteristic x-rays from the bulk; I_{co}/I_f = enhancement factor due to continuous x-rays (bremsstrahlung) from the bulk. Inserts: I_{co}/I_f and/or I_{ch}/I_f on a different scale.

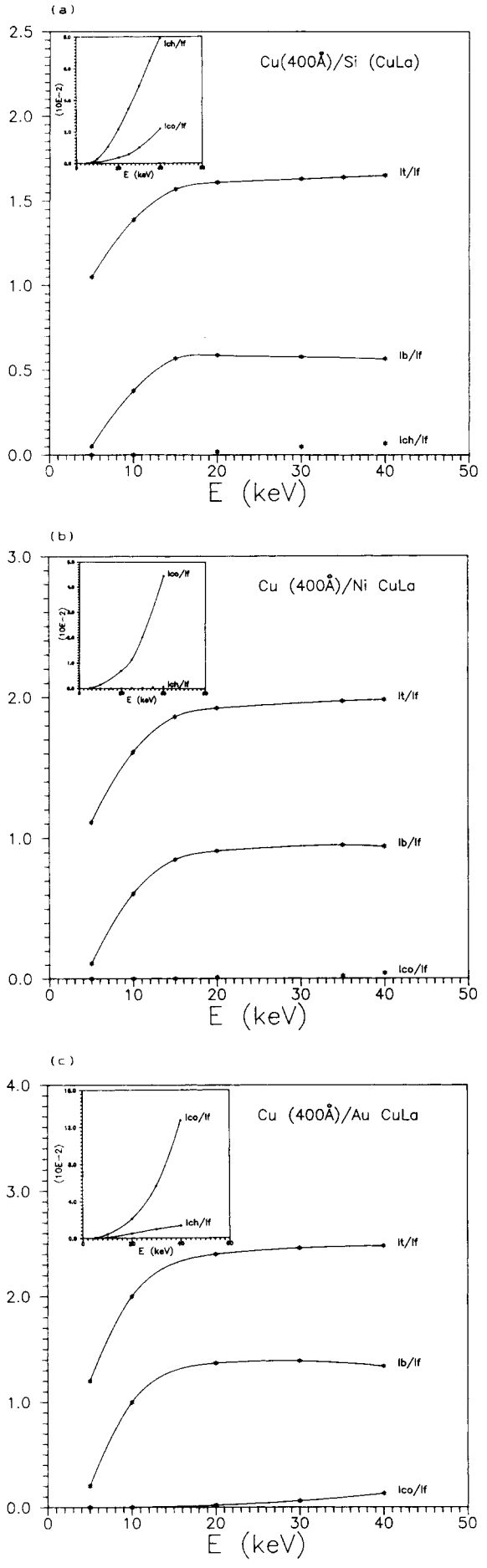

Figure 2. Same as in Fig. 1 but for Cu Lα radiation.

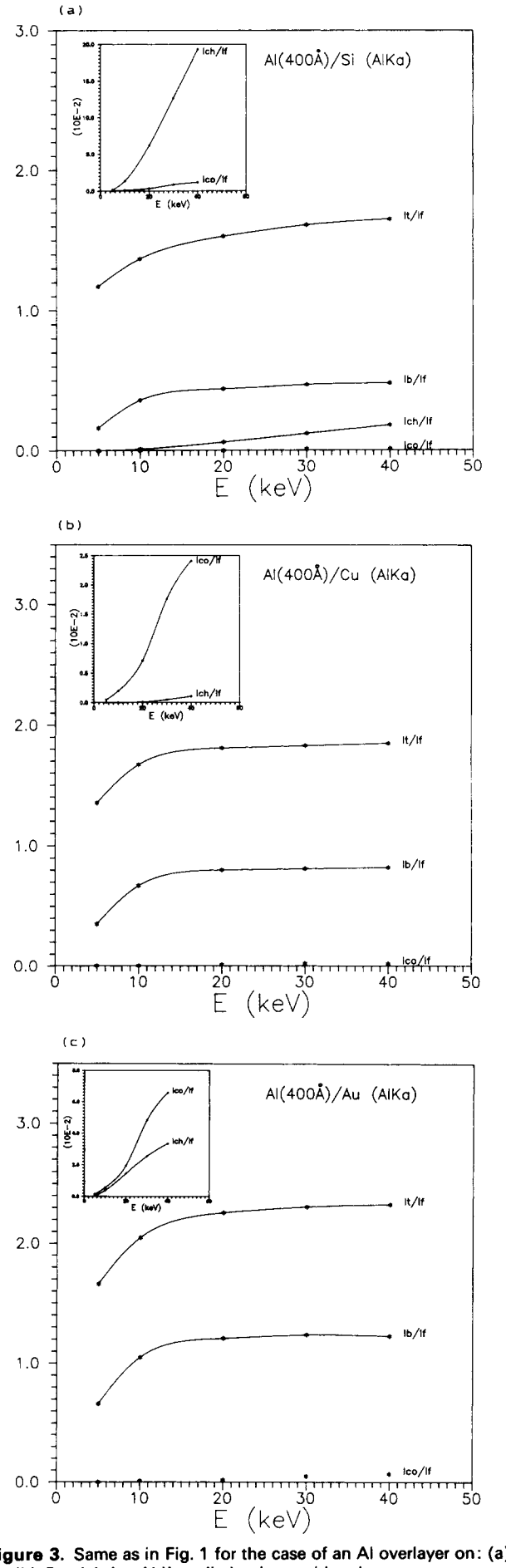

Figure 3. Same as in Fig. 1 for the case of an Al overlayer on: (a) Si; (b) Cu; (c) Au. Al Kα radiation is considered.

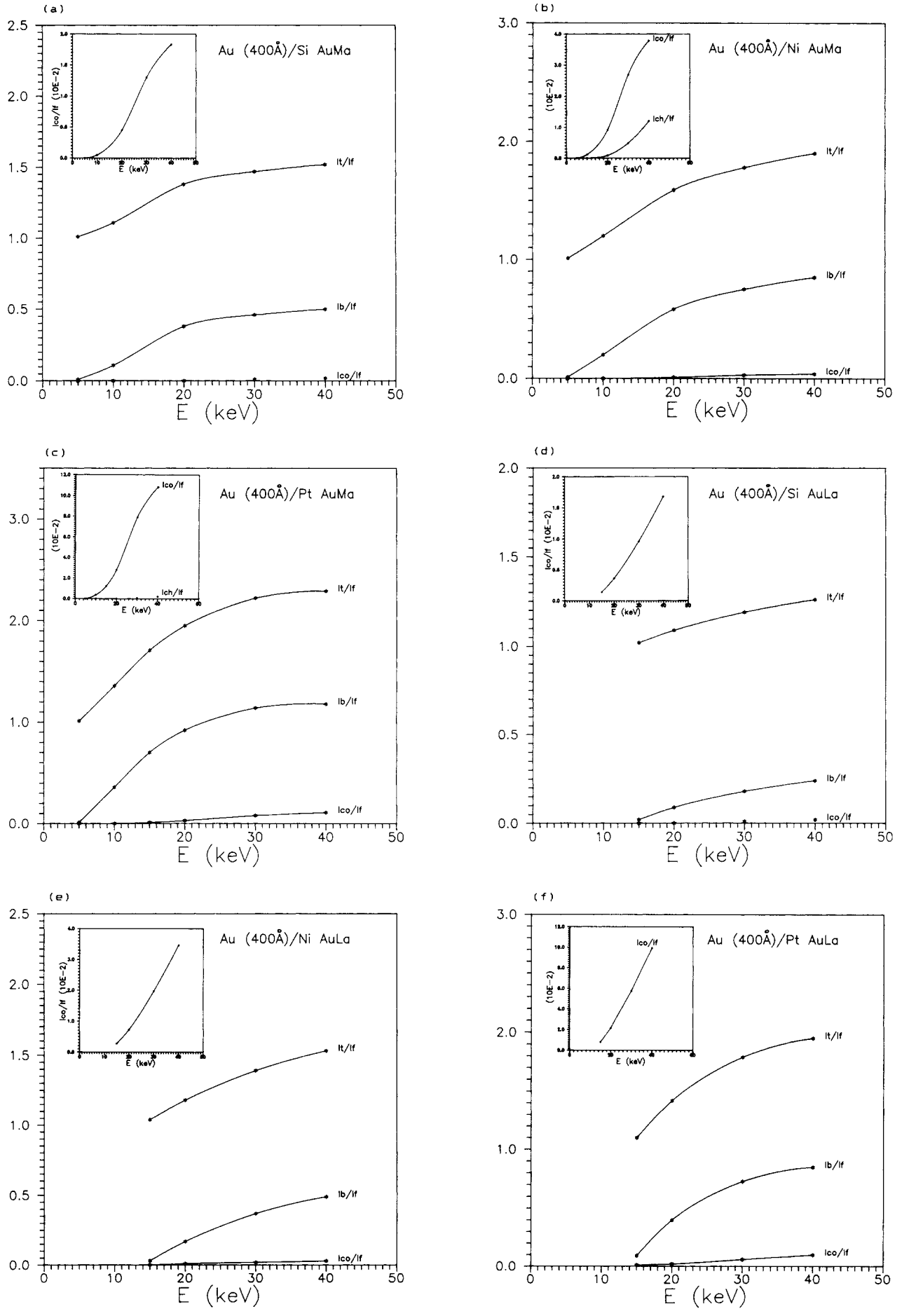

Figure 4. Same as in Fig. 1 for an Au overlayer on Si, Ni and Pt. Au Mα and Au Lα lines have been considered.

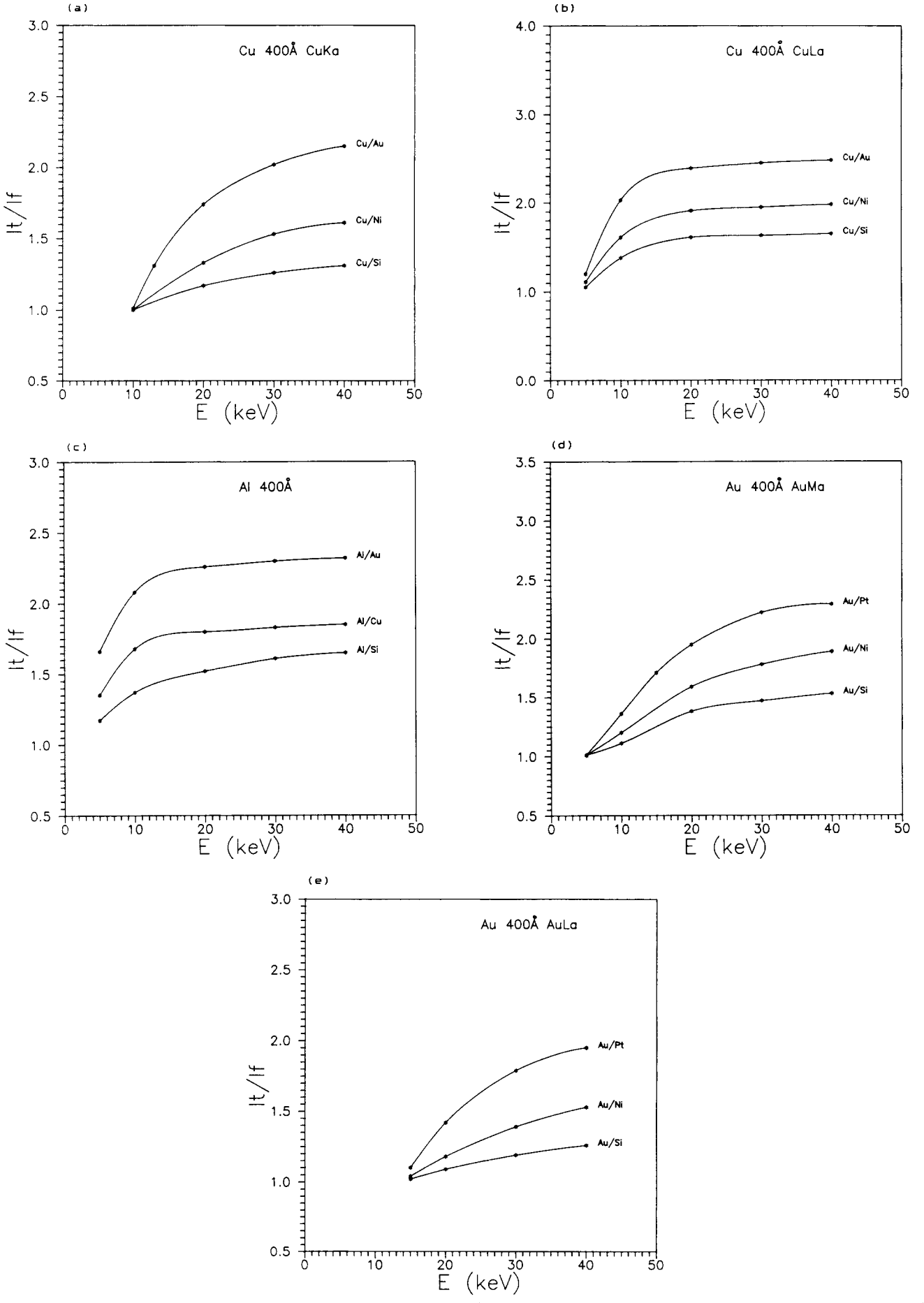

Figure 5. Comparison of I_t/I_f for different overlayers (Al, Cu, Au) on different substrates (Si, Cu, Ni, Pt, Au). I_t/I_f increases when the Z of the substrate increases. It depends also on the analysed x-radiation.

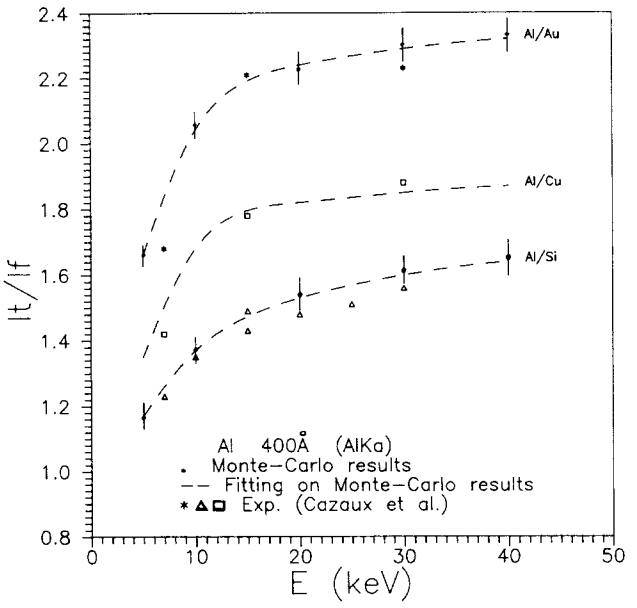

Figure 6. Comparison of results from Monte Carlo calculations with published experimental results obtained by Cazaux *et al.*:[27,28] (●) Monte Carlo calculations; (– – –) fitting on Monte Carlo calculations; (*) experimental results for the case of Al/Au; (□) experimental results for the case of Al/Cu; (△) experimental results for the case of Al/Si. The agreement between experimental results and calculations is quite good.

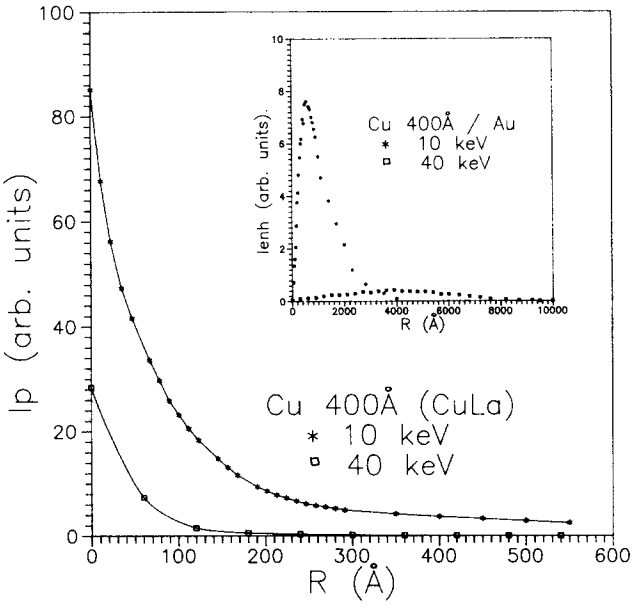

Figure 7. Main figure: lateral extent of the x-ray signal induced by the primary electron beam for a copper film (thickness 400 Å) on Au at two different primary beam energies. Insert: lateral extent of the enhancement signal induced by fluorescence and by back-scattered electrons. The lateral extent of this signal (I_{enh}) is far greater than that of the signal I_p induced by the primary beam (4000 Å instead of 250 Å at 10 keV, and 10 μm instead of 250 Å at 40 keV). On the other hand, its x-ray intensity at each point, measured with the same arbitrary units, is much smaller than that of I_p (its maximum value is of the order of 8% at 10 keV and 1.3% at 40 keV). We can conclude that the influence of the enhancement signal on the lateral resolution is minimal and less important at higher primary beam energies. The resolution is governed principally by the primary beam-induced signal.

mental set-up consisted of a thin film supported by a grid, so two regions were distinguished, one for the measurement of the signal from the unsupported film and the other for the measurement of the film on bulk. The agreement of the experimental values with our results is good if we take into account that some discrepancy may be due not only to approximations in the calculations but also to experimental error owing to difficulties in the experimental verification. Indeed, in the case of the supported film, the need is for a film of uniform thickness in good contact with the substrate, without any kind of foreign element at the interface. In the case of the unsupported film, any spurious contribution to the x-ray signal has to be avoided, so the film must be put as far as possible from its holder. On the other hand, there is an error in the calculated values; it has been estimated by taking into account the most important sources of errors as follows:

(1) An error due to the sequence of random numbers used. The discrepancy of the results has been estimated to be of the order of 0.9% of the total signal I_f/I_f in the case of Al/Au at 40 keV and 3.9% in the case of Al/Si at 40 keV.

(2) An error from the expression of the back-scattering coefficient used. The expression given by Arnal *et al.*[39] is compared to the polynomial expression by Reuter.[40] The corresponding error is of the order of 3% of the total signal I_f/I_f in the case of Al/Si at 40 keV and of the order of 1.3% of the total signal in the case of Al/Au at 40 keV. Its influence on the signal induced by back-scattered electrons is of the order of 10.7% in the first case and of the order of 2.5% in the second case.

(3) An error from the expression used for the mean ionization potential. The simple expression by Love *et al.*[12] is compared to that used (Eqn (3) above). The error is of the order of 1.5% of the total signal in the case of Al/Au at 40 keV and of the order of 0.2% in the case of Al/Si at 40 keV.

The error from the expression used for the absorption coefficient has been found to be negligible.

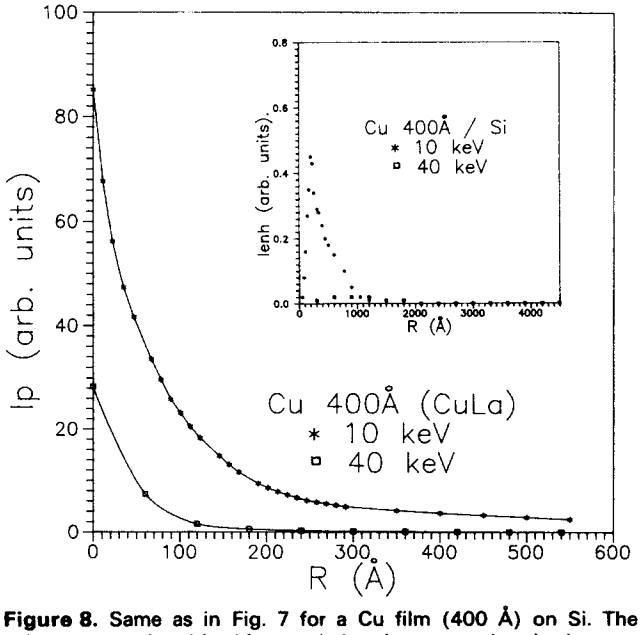

Figure 8. Same as in Fig. 7 for a Cu film (400 Å) on Si. The enhancement signal in this case is less important than in the case of an Au substrate; it thus has no influence on the lateral resolution.

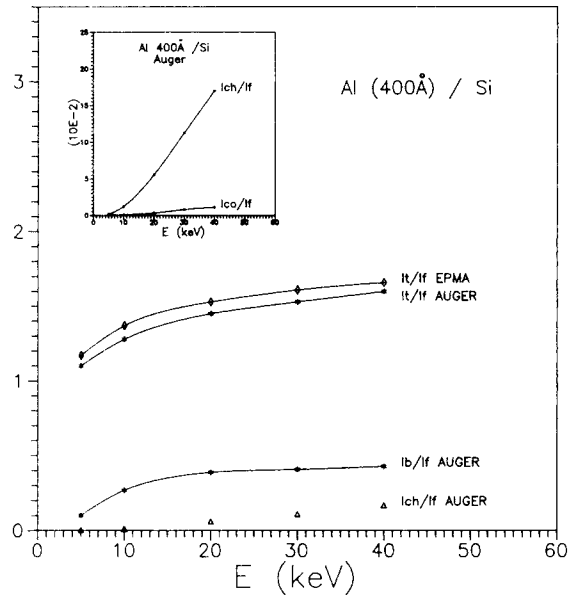

Figure 9. Results as in Fig. 1 but an Auger signal Al KLL is analysed compared to results obtained for the case of EPMA (Al Kα): (◇) EPMA (Al Kα radiation); (*) Auger (Al KLL).

Bars of the total error are indicated in the curves corresponding to Al/Au and Al/Si in Fig. 6.

The lateral extent of the x-ray signal is illustrated in Fig. 7 for a Cu film on Au and in Fig. 8 for a Cu film on Si. A point incident beam has been considered. The curves in the main figure indicate the signal induced by the primary electrons and the curves in the insert indicate the enhancement factor due to back-scattered electrons and continuous and characteristic x-rays. The same (arbitrary) units have been used in the main figure and in the insert. It is obvious that, owing to the lateral dispersion of the signals induced by fluorescence and by back-scattered electrons, the contribution of the enhancement signal at each lateral point is small (only a few per cent of the signal induced by primary electrons). Thus, by using criteria such as those of Rayleigh or Sparrow, we can conclude that the lateral resolution is mainly governed by the primary beam (see Ref. 41).

Figure 9 shows Monte Carlo results for the case of an Al film on Si obtained when the Auger signal (Al KLL) is detected (10000 trajectories were necessary in this case, instead of the 5000 trajectories in the case of EPMA, because the signal obtained is smaller). The I_i/I_f ratio is a little smaller than that obtained in EPMA.

We have compared our results concerning the fluorescence correction with those obtained by Cazaux *et al.*,[21] who have used approximate analytical formulae. Although we have not studied exactly the same films with these authors and the comparison is not direct, we can conclude by comparing approximately equivalent film/bulk systems (same difference in their Z number) that the same order of range of corrections is obtained in both cases.

Further results of the enhancement factors and additional results concerning the lateral resolution in Auger electron spectroscopy of stratified materials have been presented at the ECASIA meeting (Antibes, France, November 1989) and will appear in a special issue of this journal.[42]

CONCLUSION

It has been shown that when thin overlayers on a bulk material have to be analysed by EPMA or AES, the enhancement due to back-scattered electrons is very important at high primary energies in cases where the substrate is composed of a material of high Z value. The contribution of characteristic and continuous x-rays created in the bulk by the primary beam is also important and not negligible in some cases (a favourable x-ray cross-section for the case of the characteristic radiation, and a material of high Z value at high primary beam energies for the case of continuous radiation). In general, the contribution of the continuous radiation is $<15\%$. The influence of these three contributions to the spatial resolution when stratified materials are analysed also has been considered.

REFERENCES

1. R. Castaing, Doctoral Thesis, University of Paris (1951).
2. J. Henoc, *Nat. Bur. Stand., Spec. Publ.* **298**, 197 (1968).
3. S. J. B. Reed, *Br. J. Appl. Phys.* **16**, 913 (1965).
4. T. O. Ziebold and R. E. Ogilvie, *Anal. Chem.* **36**, 322 (1964).
5. J. Philibert and R. Tixier, *J. Phys. D., Ser. 2* **1**, 685 (1968).
6. J. L. Pouchou and F. Pichoir, *Rech. Aerosp.* **3**, 167 (1984); **5**, 349 (1984).
7. D. F. Kyser and K. Murata, *IBM J. Res. Dev.* 352, July (1974).
8. H. E. Bishop and J. C. Riviere, *J. Appl. Phys.* **40**, 1740 (1969).
9. J. Henoc, Thesis, Paris, Publication CNET No. 655 (1962).
10. J. Henoc and F. Maurice, Rapport CEA-R-4615 (1975).
11. R. Castaing and J. Descamps, *J. Phys. Radiat.* **16**, 304 (1955).
12. G. Love, M. G. C. Cox and V. D. Scott, *J. Phys. D* **10**, 7 (1977).
13. R. H. Packwood and J. D. Brown, *X-Ray Spectrom.* **10**, 138 (1981).
14. J. L. Pouchou and F. Pichoir, *12th ICXOM, Cracow* (1989), abstracts booklet, p. 14, to appear in the proceedings to be published by the Institute of Metallurgy, Academy of Metallurgy and Mining, Cracow.
15. S. Ichimura, M. Aratama and R. Shimizu, *J. Appl. Phys.* **51**(5), 2853 (1980).
16. S. Ichimura, Ding Ze-Zung and R. Shimizu, *Surf. Interface Anal.* **13**, 149 (1988).
17. A. Jablonski, *Surf. Sci.* **87**, 539 (1979); *Surf. Interface Anal.* **2**, 39 (1980).
18. J. P. Langeron, *VAMAS Project*, presented at the 5th Int. Conf. on Quantitative Surface Analysis (November 1988).
19. C. C. Chang, *J. Electron Spectrosc. Relat. Phenom.* **13**, 255 (1978).
20. J. A. D. Matthew and H. Taylor, 4th Intnl Conf. on Quantitative Surface Analysis, Teddington, UK, November 1979 (unpublished proceedings).
21. J. Cazaux and S. Moutou, *Surf. Interface Anal.* **6**(2), 62 (1984).
22. J. Cazaux, D. Gramari, S. Moutou and A. G. Nassiopoulos, *J. J. Phys.* **45**, C2–337 (1984).
23. D. Gramari and J. Cazaux, *Surf. Sci.* **136**, 83 (1983).

24. M. M. El Gomati, *Surf. Sci.* **152/153**, 877 (1985).
25. M. M. El Gomati, *Inst. Phys. Conf. Ser. No. 93* **2**, 167 (1988).
26. W. Williamson and G. C. Duncan, *Am. J. Phys.* **54**(3), 262 (1986).
27. D. C. Joy, *Inst. Phys. Conf. Ser. No. 93* **1**, 23 (1988).
28. H. Bethe, *Ann. Phys. (Leipzig)* **5**, 325 (1930).
29. M. J. Berger and S. M. Seltzer, *N.A.S.–N.R.C. Publ.* **1133**, 205 (1964).
30. T. S. Rao-Sahib and D. B. Wittry, *J. Appl. Phys.* **45**, 5060 (1974).
31. X-ray Cross-section Compilations from 0.1 keV to 1 MeV. Kaman Science Corporation, Colorado Springs, Colorado 80907.
32. N. A. Dyson, *Proc. Phys. Soc.* **73**, 924 (1959).
33. O. Jbara, X. Thomas and J. Cazaux, *12th ICXOM, Cracow* (1989), abstracts booklet, p. 227, to appear in the proceedings to be published by the Institute of Metallurgy, Academy of Metallurgy and Mining, Cracow.
34. J. Cazaux, *J. Microsc.* **145**, 257 (1987).
35. M. Tholomier, D. Dogmane and E. Vicario, *J. Microsc. Spectrom. Electron.* **13**, 119 (1988).
36. M. M. El Gomati, M. Prutton, B. Lamb and C. G. Tuppen, *Surf. Interface Anal.* **11**, 251 (1988).
37. J. Cazaux, O. Jbara and X. Thomas, *EMAS 1989* Envers, Belgium (1989).
38. J. Cazaux, O. Jbara, A. G. Nassiopoulos and E. Valamontes, *12th ICXOM, Cracow* (1989), abstracts booklet, p. 38, to appear in the proceedings to be published by the Institute of Metallurgy, Academy of Metallurgy and Mining, Cracow.
39. F. Arnal, P. Verdier and P.-D. Vincensini, *C. R. Acad. Sci.* **268**, 1526 (1969).
40. W. Reuter, *Proc. 6th Int. Conf. on X-ray Optics and Microanalysis*, p. 121. University of Tokyo Press, Tokyo (1972).
41. J. Cazaux, *Surf. Interface Anal.* (1989); paper presented at the Quantitative Surface Analysis (QSA-5) Conference, London, 15–18 November 1988.
42. E. Valamontes, A. G. Nassiopoulos and N. Glezos, *Surf. Interface Anal.* **16**, in press (1990).